Progress In Electromagnetics Research, PIER 66, 27–40, 2006

AN IMPROVED SPHERICAL ANTENNA ARRAY FOR WIDEBAND PHASE MODE PROCESSING

M. D. Huang and S. Y. Tan

School of Electrical and Electronic Engineering
Nanyang Technological University
50 Nanyang Avenue, Singapore 639798

Abstract—This paper presents an icosahedron-based spherical antenna array for phase mode processing. In this topology, the inter-element spacing is almost identical. This feature is useful for three-dimensional beam scanning and for reducing the effects of mutual coupling. The use of directional elements in this array for wideband synthesis is discussed, and our results show that the use of such elements can overcome the limitations of rapid variations in the amplitude of the far-field mode over a wide frequency band and enable such array to synthesize wideband patterns.

1. INTRODUCTION

The analysis and synthesis of circular antenna arrays has been studied using the concept of phase mode excitation over the past four decades [1–7]. The excitation of planar circular antenna arrays can be conveniently analyzed in terms of a Fourier series [1], and each term of the series is called a phase mode. When a circular array is excited by a phase mode, the far-field radiation pattern has the same phase variation with azimuth angle and a constant amplitude given by a Bessel function coefficient. These properties are mainly due to their symmetry and 360° coverage. This kind of circular antenna array can be implemented conveniently by using a Butler matrix network [2]. The use of directional elements in circular array can overcome the limitation of rapid variation in the amplitude of the far-field and allow such arrays to be used in wideband applications [3].

Recently, this concept is extended to the spherical phase mode [8] and the spheroidal phase mode [9] based on spherical and spheroidal array geometries respectively. These results show that similar characteristics to a circular phase mode have been obtained in

three-dimensions. The interest of such spherical or spheroidal antenna arrays is based on the possibility to scan a single or multiple beams through the whole three-dimensional space with low grating lobe levels [8–14]. However, spherical or spheroidal arrays based on equiangular sampling schemes can only scan the beam in the azimuth angle but not the elevation angle electrically [8, 9]. This is because the distribution of equiangular sampling scheme is not uniform in the elevation angle. Furthermore, the sampling points for such array are much denser near the poles than at the equator due to the equiangular topology, which make the array suffer severe mutual coupling effects near the poles. To take into account the effects of mutual coupling, the embedded element pattern should be used. This kind of problems have been analyzed by several papers [15–18].

The purpose of this paper is to present an improved topology (based on an icosahedron) of spherical antenna arrays for phase mode processing in order to overcome the above-mentioned limitations. In this icosahedron-based topology, the inter-element spacing is almost identical. This attractive property can be used for three-dimensional beam scanning and for reducing the effects of mutual coupling. The use of directional elements in this array is discussed which shows that the amplitude of the far-field mode does not go to zero for any frequency so that this proposed array can be used for wideband synthesis.

2. TOPOLOGY

A spherical antenna array with equal separation between neighboring elements is desirable for three-dimensional beam scanning and for reducing the effects of mutual coupling. Designing such an array is equivalent to the problem of symmetrically dividing a spherical surface about a center point into areas of congruent polygons. The geometry so formed is a regular polyhedron [19]. However, there are only five regular polyhedra, i.e., tetrahedron, cube, octahedron, dodecahedron and icosahedron [20]. Each polyhedron has an inscribed sphere and a circumscribing sphere, the spheres being concentric. The best angular resolution among the five regular polyhedra is given by the icosahedron [19], which has 12 vertices, 20 equilateral triangular faces and 30 edges as shown in Fig. 1.

To increase the number of array elements, each equilateral triangle can be subdivided into a number of smaller equilateral triangles in terms of subdivision scheme named 'alternative breakdown scheme with frequency v' [21] as shown in Fig. 1, where v is the number of subdivisions of the edge of the equilateral triangle. The number of the

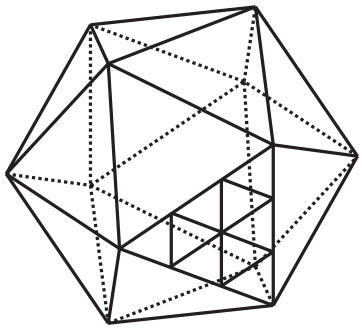

Figure 1. Icosahedron with a subdivision scheme ($v = 3$) on one face.

vertices of all the subdivided triangles N can be calculated by

$$N = 10v^2 + 2 \tag{1}$$

However, this is an approximate method in the sense that when these vertices are projected onto the inscribed or circumscribing sphere, the separation between neighboring elements is no longer exactly the same. This is because the vertices are now located at various points in between the inscribed and circumscribing sphere, instead of all lying on the circumscribing sphere for the original icosahedron.

In order to obtain equal distance between elements on the surface of the inscribed or circumscribing sphere, the vertices on the triangular surface need to be rearranged before mapping to the spherical surface. Unfortunately, it is a well-known group-theoretical result that there are no completely uniform distribution on the sphere for $N > 20$ [22]. In this paper, we make use of the method of area equalization [22] to obtain approximately equal distance. Without loss of generality, we assume an inscribed sphere with radius a. Since each face of the icosahedron can be projected onto a region on the inscribed sphere bounded by three great circles, and any face of this circumscribing icosahedron can be rotated to lie in the $z = a$ plane by multiplying an appropriate rotation matrix. Therefore, we only need to consider this triangular face. The area equalization is to find a mapping, $(x, y, a) \rightarrow (x', y', a)$, on this triangular face whose Jacobian is proportional to the inverse of the Jacobian of the mapping from the inscribed unit sphere to the triangular plane, where (x, y, a) and (x', y', a) denote the coordinates of the vertices before and after mapping respectively. Therefore, the Jacobian of these two mappings is a constant, and this combined mapping is a equal-area mapping. Because the Jacobian of the mapping from the sphere to the plane is $(\frac{a^2+x^2+y^2}{a^2})^{\frac{3}{2}}$, the mapping

$(x, y, a) \rightarrow (x', y', a)$ should satisfy the nonlinear partial differential equation

$$\det \begin{pmatrix} \partial x'/\partial x & \partial x'/\partial y \\ \partial y'/\partial x & \partial y'/\partial y \end{pmatrix} = C\Big(\frac{a^2 + x^2 + y^2}{a^2}\Big)^{-\frac{3}{2}} \tag{2}$$

where C is a proportionality constant of mapping which is the ratio of the area of the triangle to the area of the triangular region mapping on the inscribed sphere and is given by

$$C = \frac{\frac{\sqrt{3}}{4}[9\tan^2(\frac{\pi}{5}) - 3]a^2}{\frac{4\pi a^2}{20}} \approx 1.21$$

Solving the partial differential equation (2), the coordinates of the vertices after mapping, (x', y', a), can be calculated by the following equations

$$\begin{cases} y' &= a\sqrt{\dfrac{2C}{\sqrt{3}}\tan^{-1}\Big[\sqrt{3}\dfrac{\sqrt{a^2+4y^2}-a}{\sqrt{a^2+4y^2}+3a}\Big]} \\ x' &= \Big(\dfrac{xy'}{y}\Big)\sqrt{\dfrac{a^2+4y^2}{a^2+x^2+y^2}} \end{cases} \tag{3}$$

After projecting these adjusted vertices (x', y', a) onto the inscribed sphere surface, and by placing an antenna element on each vertex, an icosahedron-based spherical antenna array is obtained which can provide approximately equal distance between the neighboring elements. The average distance between the neighboring elements d is approximately given by

$$d \approx \frac{3.81a}{\sqrt{N}} \tag{4}$$

3. SPHERICAL ANTENNA ARRAYS

3.1. Spherical Phase Mode

The spherical phase modes or spherical harmonics are the angular portion of the solution to the Helmholtz's or the space-dependence of the electromagnetic wave equation in spherical coordinates, which

is defined in [8] as

$$Y_l^m(\theta,\phi) = \sqrt{\frac{(2l+1)(l-m)!}{4\pi(l+m)!}} P_l^m(\cos\theta) e^{jm\phi} \tag{5}$$

where θ and ϕ are respectively the polar and azimuthal coordinates in spherical coordinate system, l is the degree of the spherical phase mode, $j = \sqrt{-1}$. P_l^m are the associated Legendre functions which means the standing spherical waves in θ and the exponential term $e^{jm\phi}$ means the travelling spherical waves in ϕ [23].

Due to the completeness property of spherical phase mode, any square integrable function $f(\theta,\phi)$ over the surface of the sphere can be expanded in a double series of spherical phase modes, which is given by [24]

$$f(\theta,\phi) = \sum_{l=0}^{\infty} \sum_{m=-l}^{l} f_{ml} Y_l^m(\theta,\phi) \tag{6}$$

and the coefficients f_{ml} can be obtained using spherical Fourier transform

$$f_{ml} = \iint_s f(\theta,\phi) Y_l^{m*}(\theta,\phi) ds \tag{7}$$

where ds is the element of the solid angle. Therefore, an excitation function on the surface of a sphere can be expressed as a linear combination of spherical phase modes.

For illustration, consider one spherical phase mode $Y_{l'}^{m'}$ as the excitation function, and the corresponding far-field radiation pattern can be represented by

$$D(\theta,\phi) = \frac{1}{4\pi} \iint_{s'} Y_{l'}^{m'}(\theta',\phi') e^{j\vec{\beta}\cdot\vec{a}} ds' \tag{8}$$

where a is the radius of the sphere, the direction of $\vec{a}$ is (θ',ϕ'), the wavenumber $\beta = 2\pi/\lambda$, the direction of $\vec{\beta}$ is (θ,ϕ). And (8) can be finally expressed by [8]

$$D(\theta,\phi) = j^{l'} j_{l'}(\beta a) Y_{l'}^{m'}(\theta,\phi) \tag{9}$$

where $j_{l'}(\beta a)$ is a spherical Bessel function of the first kind. (9) shows that the far-field radiation pattern has the same spherical phase mode form as the excitation function.

3.2. Directional Element Pattern

Although it is possible to obtain any desired far-field radiation pattern in three-dimension by means of breaking the pattern down into a series of spherical harmonics and exciting each of them around spherical array with appropriate coefficients separately, (9) shows that the amplitude of the far-field mode $j_{l'}(\beta a)$ vary rapidly with a/λ, which means the array is narrowband. [8] anticipate that the raised cosine pattern would be optimum directional element pattern with spherical phase mode excitations, and [3, 1] show that the use of directional elements can overcome the similar problem in circular antenna arrays. Our theoretical calculations show that the use of directional elements can overcome these limitations and give almost the same amplitudes of the far-field mode excited by different spherical phase modes. The simulation results will be given in Section 4.

Let us assume that the individual element pattern is raised cosine pattern $(1 + \cos\psi)$ rotated around the normal axis of the elements on the sphere (a pencil-beam radiation pattern), where ψ is the angle between $\vec{a}$ and $\vec{\beta}$. And each element has θ (or ϕ) polarization. The far-field radiation pattern excited by spherical phase mode $Y_{l'}^{m'}(\theta', \phi')$ can be represented by

$$\vec{D}(\theta, \phi) = \hat{\theta}\frac{1}{4\pi}\iint_{s'}(1 + \cos\psi)Y_{l'}^{m'}(\theta', \phi')e^{j\vec{\beta}\cdot\vec{a}}ds' \tag{10}$$

The plane wave in the far-field can be expressed by

$$e^{j\vec{\beta}\cdot\vec{a}} = \sum_{l=0}^{\infty}(2l + 1)j^l j_l(\beta a)P_l(\cos\psi) \tag{11}$$

Differentiating both side of (11) with respect to βa,

$$j\cos\psi e^{j\vec{\beta}\cdot\vec{a}} = \sum_{l=0}^{\infty}(2l + 1)j^l\frac{d}{d(\beta a)}j_l(\beta a)P_l(\cos\psi) \tag{12}$$

and using the spherical harmonic addition theorem [25],

$$P_l(\cos\psi) = \frac{4\pi}{2l + 1}\sum_{m=-l}^{l}Y_l^{m*}(\theta', \phi')Y_l^m(\theta, \phi) \tag{13}$$

we can get,

$$(1+\cos\psi)e^{j\vec{\beta}\cdot\vec{a}} = 4\pi\sum_{l=0}^{\infty}\sum_{m=-l}^{l} j^l\Big(j_l(\beta a) - j\frac{d}{d(\beta a)}j_l(\beta a)\Big) \cdot Y_l^{m*}(\theta',\phi')Y_l^m(\theta,\phi) \tag{14}$$

Substituting (14) into (10), and using the orthogonality property of spherical harmonics over the sphere [25],

$$\iint_s Y_{l_1}^{m_1*}(\theta,\phi)Y_{l_2}^{m_2}(\theta,\phi)ds = \delta_{l_1,l_2}\delta_{m_1,m_2} \tag{15}$$

The far-field radiation is obtained as,

$$\vec{D}(\theta,\phi) = \hat{\theta}j^{l'}\Big(j_{l'}(\beta a) - j\frac{d}{d(\beta a)}j_{l'}(\beta a)\Big)Y_{l'}^{m'}(\theta,\phi) \tag{16}$$

Comparing with (9), (16) shows that a spherical array with directional element pattern excited by a spherical phase mode also leads to a far-field radiation pattern with the same phase mode. But the amplitude of the far-field mode is no longer a single spherical Bessel function but is a sum of such functions, which prevents the amplitude going to zero for any value of βa. Furthermore, for electrically large spherical arrays ($\beta a \gg l(l+1)/2$), the asymptotic expansions of spherical Bessel functions can be used [25],

$$j_l(x) \approx \frac{1}{x}\sin\left(x - \frac{l\pi}{2}\right) \tag{17}$$

and

$$\frac{d}{dx}j_l(x) \approx \frac{1}{x}\cos\left(x - \frac{l\pi}{2}\right) \tag{18}$$

Therefore the far-field radiation pattern becomes

$$\vec{D}(\theta,\phi) = \hat{\theta}\frac{1}{(\beta a)}e^{j(\beta a - \frac{\pi}{2})}Y_{l'}^{m'}(\theta,\phi) \tag{19}$$

(19) shows that for electrically large arrays the amplitude of the far-field mode is inversely proportional to frequency, and do not have any nulls. Furthermore, the amplitude does not depend on the degree of the exciting spherical phase mode, which means that the use of such directional element pattern can give almost the same amplitudes of the

far-field mode excited by different spherical phase modes for electrically large arrays. In addition, the phase of the far-field mode only varies with frequency linearly. Therefore, a linear coefficient with frequency in both amplitude and phase, such as $(\beta a e^{-j\beta a})$, can be added to the excitation functions in order to compensate this decay, and keep the same radiation pattern in a wide bandwidth.

3.3. Icosahedron-based Arrays

For the spherical arrays, N elements will be set in terms of preceding method presented in Section 2. The excitation at each element will be the value of the spherical harmonic Y_l^m at the coordinates of the element $(a_i = a, \theta_i, \phi_i)$, $i = 1, ..., N$, which can be considered as a product of Y_l^m with a spatial sampling function $S(\theta, \phi)$. The sampling function for this distribution is given as follows,

$$S(\theta, \phi) = \sum_{i=0}^{N-1} w_i \delta_{(\theta_i, \phi_i)} \tag{20}$$

where the weights w_i of the array elements are all the same due to the symmetry of the topology, and given by

$$w_i = \frac{4\pi}{N}, \quad i = 1, ..., N \tag{21}$$

and the far-field radiation pattern (8) can be rewritten by

$$\begin{aligned} D(\theta, \phi) &= \frac{1}{4\pi} \sum_{i=0}^{N-1} w_i Y_l^m(\theta_i, \phi_i) e^{j\vec{\beta}\cdot\vec{a}_i} \\ &= \frac{1}{N} \sum_{i=0}^{N-1} Y_l^m(\theta_i, \phi_i) e^{j\vec{\beta}\cdot\vec{a}_i} \end{aligned} \tag{22}$$

When a spherical harmonic is excited in this array distribution, there will be other harmonics radiating in the far-field, which distort the far-field pattern. Our calculations show that when the inter-element spacing d given in (4) is small, e.g., $d < \lambda/2$, or equivalently the number of array elements $N > 58(a/\lambda)^2$, the distortion of this icosahedron-based topology is negligible. In this condition, if rotated raised cosine pattern elements are used in an electrically large icosahedron-based array as mentioned in Section 3.2, The far-field pattern becomes,

$$\vec{D}(\theta, \phi) \approx \hat{\theta} \frac{1}{(\beta a)} e^{j(\beta a - \frac{\pi}{2})} Y_l^m(\theta, \phi) \tag{23}$$

The amplitude and the phase variance with frequency also can be compensated by multiplying a appropriate coefficient, such as $(\beta a e^{-j\beta a})$, which is presented in Section 3.2. Therefore, this icosahedron-based arrays can be used to wideband applications with the concept of spherical phase mode processing, such as UWB systems.

4. RESULTS AND DISCUSSION

Fig. 2 shows the far-field radiation patterns excited by a spherical phase mode Y_3^2, with $a/\lambda = 3.33$ and the number of the array elements $N = 3612$ ($v = 19$ in (1)) for the comparison with the results in [8] with $N = 4096$. It shows that the pattern for this icosahedron-based antenna array is practically the same as the theoretical pattern in [8] for both amplitude and phase.

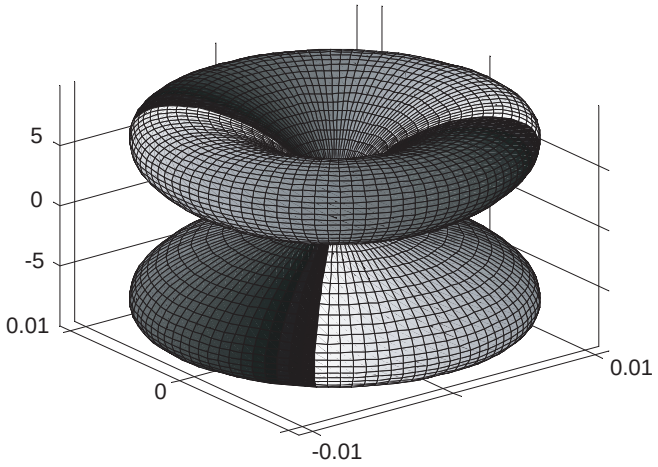

Figure 2. Far-field radiation pattern of icosahedron-based antenna array excited by spherical phase mode Y_3^2 with $a/\lambda = 3.33$ and $N = 3612$. (phase is represented on gray scale)

Fig. 3(a) and 3(b) show the amplitudes of the far-field mode excited by spherical phase mode Y_1^0 and Y_3^2 versus a/λ for both isotropic element pattern and the rotated raised cosine pattern respectively in the case of zero inter-element spacing. It can be noticed that the nulls are cancelled due to the effect of the directional pattern. This is because in (16), $j_l'(\beta a)$ is approximately a maximum when $j_l(\beta a) \to 0$, and vice versa (except for $\beta a \to 0$ when $l > 1$). Therefore, the concept of spherical phase mode can be used for wideband synthesis.

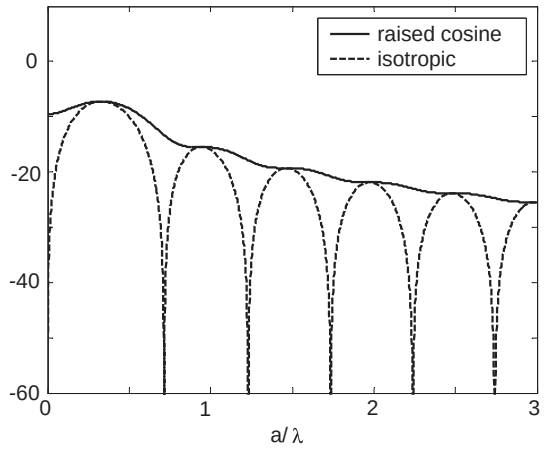

(a) Y_1^0

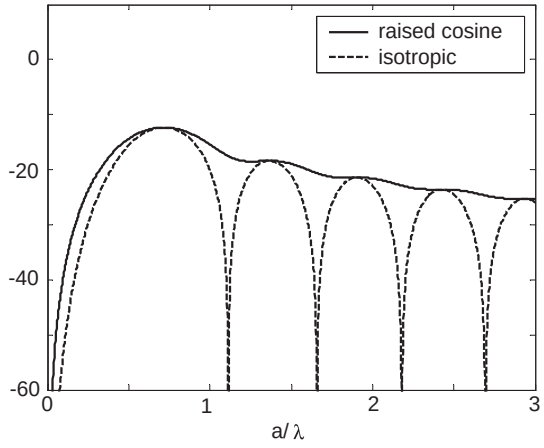

(b) Y_3^2

Figure 3. Amplitudes of the far-field mode excited by spherical phase modes Y_1^0 and Y_3^2 versus the radius of array in wavelengths a/λ.

Fig. 4 shows the amplitudes of the far-field mode excited by spherical phase mode Y_3^2 versus a/λ for both zero inter-element spacing case and icosahedron-based topology case respectively with rotated raised cosine element pattern. The number of array elements are $N = 812$ ($d/a \approx 0.134$) and $N = 256$ ($d/a \approx 0.238$) respectively. It shows that the use of directional elements prevents the amplitude of the far-field mode going to zero. And it is also seen that the far-field patterns of the icosahedron-based array are approximately the

same as the zero spacing array up to $a/\lambda \approx 4$, i.e. $d/\lambda \approx 0.5$ for $N = 812$ and to $a/\lambda \approx 2$, i.e. $d/\lambda \approx 0.5$ for $N = 256$. This is because when $d/\lambda < 0.5$, the distortion terms are negligible as presented in the last section. When $d/\lambda > 0.5$ for the case $N = 256$, the difference between the results of the zero-spacing array and icosahedron-based array become larger and larger.

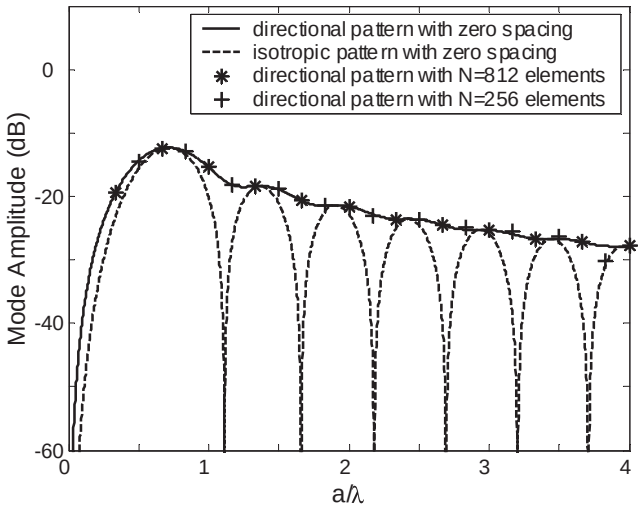

Figure 4. Amplitudes of the far-field mode excited by Y_3^2 versus a/λ for $N = 812$ and $N = 252$ with rotated raised cosine element pattern.

Fig. 5 shows the amplitudes of the far-field mode excited by Y_1^0 with rotated raised cosine element pattern for $a/\lambda = 10.0$ and $d/\lambda \approx 0.3$ at 6.0 GHz with a compensation coefficient ($\beta a e^{-j\beta a}$). It shows that with the compensation, the amplitudes of the far-field mode are practically the same in a wide bandwidth (2–11 GHz). This is because when the frequency is large, e.g., 2 GHz, the antenna array can be seen as an electrically large array. Therefore, the icosahedron-based array with directional element can be used in wideband synthesis with spherical phase mode processing including UWB (3.1–10.6 GHz) applications.

Because of the symmetry of the icosahedron-based antenna array, it is possible to scan the beam electronically in the whole 4π steradians of the space by rotating the excitation distribution through appropriate polar and azimuth angle. Therefore, a number of applications, such as broadband pattern synthesis, null steering, direction finding, and superresolution presented in [4–7], can be used in both azimuth and elevation angle.

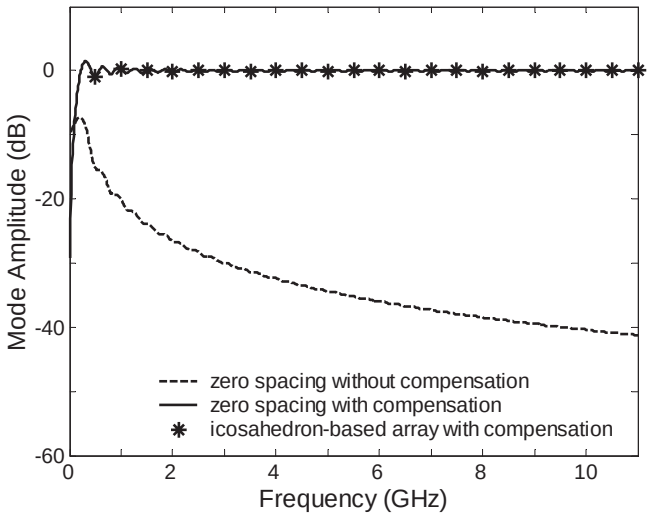

Figure 5. Compensated amplitudes of the far-field mode excited by Y_1^0 with rotated raised cosine element pattern for $a/\lambda = 10.0$ and $d/\lambda \approx 0.3$ at 6.0 GHz.

Furthermore, all of antenna arrays suffer from the mutual coupling effects, and these detrimental effects intensify as the space between elements is decreased. As mentioned before, the effects of the mutual coupling are so severe near the poles of the array using the equiangular grid that the radiation pattern would be strongly affected. But for the icosahedron-based topology, the elements distribution on the sphere are almost uniform which can reduce the effects of mutual coupling.

5. CONCLUSION

An improved spherical antenna array has been presented in this paper. Our results show that this icosahedron-based topology can be used for phase mode processing. To overcome the limitations of rapid variations in the amplitude of the far-field mode, the rotated raised cosine pattern elements are used in this array, which enables us to synthesize a wideband pattern without moving nulls. And a number of attractive properties for applications are discussed such as electric beam scanning in the whole three-dimensional space and reducing the effects of mutual coupling.

ACKNOWLEDGMENT

The authors would like to thank Prof. Max Tegmark for providing the valuable code package to generate the coordinates of the vertices of the icosahedron-based topology used in this paper.

REFERENCES

1. Davies, D. E. N., *The Handbook of Antenna Design*, Ch. 12, Peter Peregrinus, Stevenage, 1983.
2. Davies, D. E. N., "A transformation between the phasing techniques required for linear and circular aerial arrays," *Proc. IEE*, Vol. 112, No. 11, 2041–2045, 1965.
3. Rahim, T. and D. E. N. Davies, "Effect of directional elements on the directional response of circular antenna arrays," *Proc. IEE*, Vol. 129, Pt. H, No. 1, 18–22, 1982.
4. Griffiths, H. D., N. Karavassilis, M. R. Jones, and D. E. N. Davies, "Broadband nulls from a circular array," *Proc. 4th IEE Intl. Conf. Antennas Propag.*, 1064–1076, Coventry, UK, Apr. 1985.
5. Jones, M. R. and H. D. Griffiths, "Broadband pattern synthesis from a circular array," *Proc. 6th IEE Intl. Conf. Antennas Propag.*, 55–59, Coventry, UK, Apr. 1989.
6. Griffiths, H. D. and R. Eiges, "Sectoral phase modes from circular antenna arrays," *Electron. Lett.*, Vol. 28, No. 17, 1581–1582, 1992.
7. Eiges, R. and H. D. Griffiths, "Mode-space spatial spectral estimation for circular arrays," *IEE Proc. Radar, Sonar Navig.*, Vol. 141, No. 6, 300–306, 1994.
8. De Witte, E., H. D. Griffiths, and P. V. Brennan, "Phase mode processing for spherical antenna arrays," *Electron. Lett.*, Vol. 39, No. 20, 1430–1431, 2003.
9. Huang, M. D. and S. Y. Tan, "Spheroidal phase mode processing for antenna arrays," *J. Electromagn. Waves Appl.*, Vol. 19, No. 11, 1431–1442, 2005.
10. Sengupta, D. L., T. M. Smith, and R. W. Larson, "Radiation characteristics of a spherical array of circularly polarized elements," *IEEE Trans. Antennas Propagat.*, Vol. 16, No. 1, 2–7, 1968.
11. Tomasic, B., J. Turtle, and S. Liu, "A geodesic sphere phased array for satellite control and communication," *Proc. URSI XXVIIth General Assembly*, Maastricht, The Netherlands, 2002.
12. Sipus, Z., N. Burum, and J. Bartolic, "Analysis of rectangular

microstrip patch antennas on spherical structures," *Microwave Opt. Tech. Lett.*, Vol. 36, No. 4, 276–280, 2003.

13. Verhaevert, J., E. Van Lil, and A. Van de Capelle, "Uniform spherical distributions for adaptive array applications," *IEEE Vehic. Technol. Conf. (VTC'01 Spring)*, Vol. 1, 98–102, Rhodes, Greece, May 2005.
14. Yin, W. Y., L. W. Li, and M. S. Leong, "The near- and far-zone fields of periodic spherical arrays of dipole antennas on spherical chiral substrates," *Progress In Electromagnetics Research*, PIER 25, 239–260, 2000.
15. Hessel, A., Y.-L. Liu, and J. Shmoys, "Mutual admittance between two circular apertures on large conducting sphere," *Radio Sci.*, Vol. 14, No. 1, 35–41, 1979.
16. Lee, K. C., "A genetic algorithm based direction finding technique with compensation of mutual coupling effects," *J. Electromagn. Waves Appl.*, Vol. 17, No. 11, 1613–1624, 2003.
17. Burum, N., Z. Sipus, and J. Bartolic, "Mutual coupling between spherical-rectangular microstrip antennas," *Microwave Opt. Tech. Lett.*, Vol. 40, No. 5, 387–391, 2004.
18. De Witte, E., P. V. Brennan, and H. D. Griffiths, "Mutual coupling analysis of a spherical array antenna," *IASTED Conf. on Antennas, Radar and Wave Propagat.*, 324–329, Banff, Alberta, Canada, July 2005.
19. Tan, S. Y. and H. S. Tan, "Modelling and measurements of channel impulse response for an indoor wireless communication system," *IEE Proc. Microw. Antennas Propag.*, Vol. 142, No. 5, 405–410, 1995.
20. Gheorghiu, A. and V. Dragomir, *Geometry of Structural Forms*, Applied Science, London, 1978.
21. Bondyopadhyay, P. K., "Geodesic sphere phased arrays for LEO satellite communications," *Proc. IEEE AP-S Int. Symp.*, 206–209, Salt Lake City, UT, July 2000.
22. Tegmark, M., "An icosahedron-based method for pixelizing the celestial sphere," *ApJ. Lett.*, Vol. 470, 81–84, 1996.
23. Rafaely, B., "Analysis and design of spherical microphone arrays," *IEEE Trans. Speech Audio Process.*, Vol. 13, No. 1, 135–143, 2005.
24. Driscoll, J. R. and D. M. Dennis, Jr., "Computing Fourier transforms and convolutions on the 2-sphere," *Adv. Appl. Math.*, Vol. 15, 202–250, 1994.
25. Arfken, G. B. and H. J. Weber, *Mathematical Methods for Physicists*, 5th edition, Academic, San Diego, CA, 2001.